Note II
9 November 1965

Magnetic Shielding by Cubical Conducting Mesh Enclosures

Capt Bronius Cikotas Lt Donald R. Marston
Air Force Weapons Laboratory

Abstract

Theoretical expressions, derived by E. D. Sunde of BTL for calculating the shielding offered by a cubical, metal structure to CW magnetic fields, are presented. Calculations from this theory are applied to 8 ft. x 8 ft. x 8 ft. cubical structures, constructed from metal mesh, in which magnetic field shielding measurements were made. The data from the shielding measurements and the results of the theoretical calculations were in good agreement for field frequencies up to 20 Kc. This result indicates that the magnetic shielding of cubical, metal structures may be predicted from Sunde's theory for field frequencies up to 20 Kc.

I. Introduction

The shielding of volumes of space from external electric and magnetic fields by metallic structures has been a problem of interest for many years. Much work on this problem has been limited to the shielding from static fields and the shielding by idealized structures (e.g. spheres and infinite cylinders).

However, with the discovery of the large pulsed electromagnetic fields emitted by a nuclear weapon, it became desirable to study the shielding provided by practical structures from large electromagnetic fields varying rapidly with respect to time. The first step in this extensive study is to examine the shielding provided by a cubical structure constructed of metal.

E. D. Sunde, in his paper "Switching Center Shielding Against Atmospheric Induction"[1] examines the electric and magnetic shielding offered by metal hollow cylinders of finite length. He extended this work to determine the shielding produced by a hollow rectangular structure of square cross-section by equating the structure to an equivalent finite cylinder.

To test this theory, AFWL, with the help of Mr. Durand of BTL and the RCAF, measured the magnetic shielding produced by two metal mesh hollow cubes. The cubes, one made of aluminum mesh and the other of copper mesh, were 8 ft. x 8 ft. x 8 ft. They were placed in the middle of a specially constructed solenoid with a square cross-section. CW magnetic fields with frequencies as high as 20 KC were generated by the solenoid.

The measurements from this test were compared with theoretical calculations from Sunde's theory, using the known electrical and dimensional parameters of the cubes.

II. Theory

E. D. Sunde has extended his calculations[1] of the shielding afforded by a cylindrical solenoid to the approximate shielding by a cubical structure made of square wire mesh.

The shielding factor, as defined by Sunde, is given by the equation,

$$\eta = \frac{I}{I_o}$$

where

I_o is the intensity of the magnetic field in the center of the enclosure in the absence of the shielding material,

and I is the intensity of the magnetic field at the center of the shielded enclosure.

The attenuation in db is given by:

$$\text{Atten (db)} = 20 \log_{10} \frac{1}{\eta}$$

---

1. Bell Telephone Laboratories Technical Memorandum MM-63-3241-12, 27 June 1963.

The mesh used was not a square mesh, nor was it made of round wires. Therefore, certain approximations have to be made in extending Sunde's theory. Note Figures 1 and 2.

In 1 'd' is the mesh spacing. However, in 2 the mesh spacing, in approximation, is taken as the width of the repeatable unit within the mesh; which fits well with the square mesh situation. Note in Figure 2 that the spacing varies with the orientation of the mesh. Also given are the ideal and actual cross-sections of the mesh wire. The effective conductor diameter 'd_o' in figure 2 is determined by equating the cross-sectional area of the mesh wire with the area of a circle of diameter 'd_o', or:

$$d_o = (4ab/\pi)^{1/2} = 6.32 \times 10^{-3} \text{ meter}$$

As Sunde's theory was based on a cylindrical shielded structure, it incorporates the effective diameter of the enclosure 'D'. For a structure with a square cross-section of width 'S', the diameter is given by:

$$D = \frac{4S}{\pi}$$

from equating the actual circumferences with the circumferences of a circle. For the 8' x 8' x 8' enclosure used, S = 8' = 2.44 meters; which gives D = 3.11 meters. The length of the 'solenoid' in this case is also 2.44 meters.

Three correction factors, A, B, and K (as used by Sunde) must be considered in any solenoid inductance and interaction problem. These constants correct for non-ideal solenoids, and will be present in the relations for shielding (See Figures 3, 4, and 5).

The internal impedance Z_i of the wire mesh is dependent on the frequency of the signal as follows:

$$\left|\frac{\gamma_o d_o}{4}\right| \leq 1, \text{ then } Z_i = r_o$$

$$\left|\frac{\gamma_o d_o}{4}\right| > 1, \text{ then } Z_i = \frac{r_o \gamma_o d_o}{4}$$

where γ_o is the propagation constant of the electromagnetic wave in the given conducting material and r_o is the resistance per unit length of the mesh conductors. The propagation constant is given by:

$$\gamma_o = (j\omega\mu\sigma)^{1/2}$$

where ω is the radian frequency of the signal,

$\mu = \mu_r\, 4\pi \times 10^{-7}$ mks unit is the magnetic permittivity of the given shielding material,

μ_r is the relative permittivity of the shielding material (approximately equal to 1.0 for all but the ferromagnetic materials),

and σ is the conductivity of the shielding material.

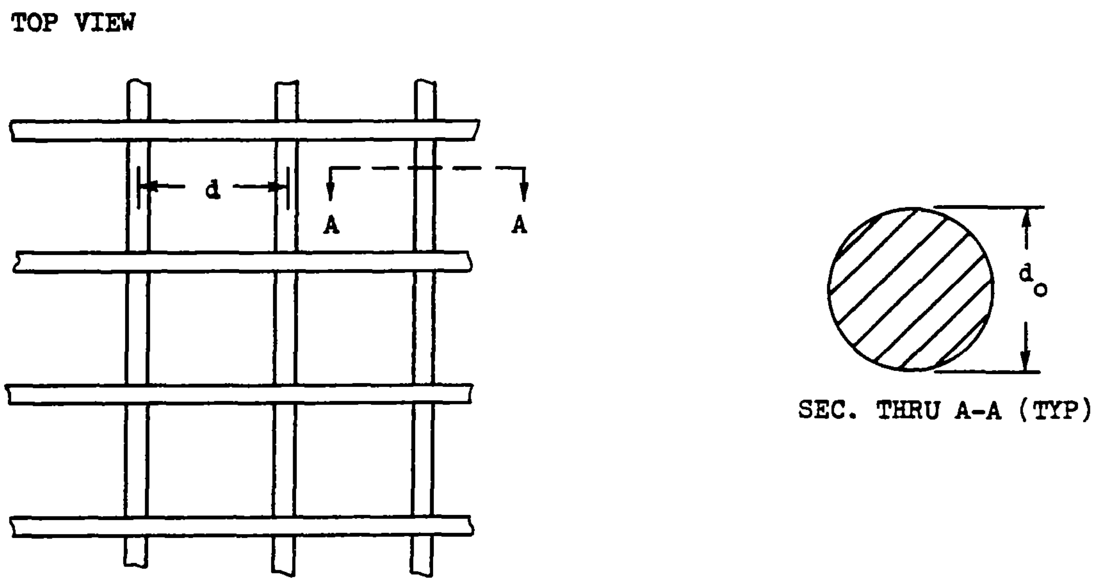

Figure 1. Mesh Used in Theoretical Development (Square Mesh, Round Cross-Section)

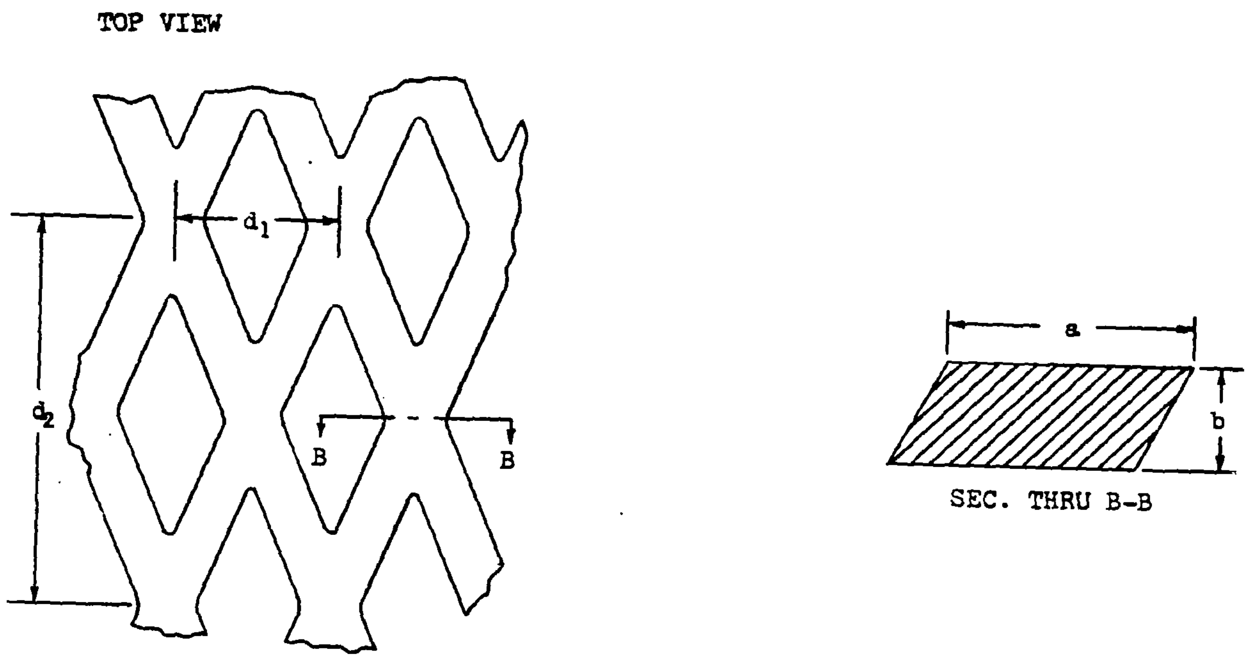

Figure 2. Mesh Used in AFWL-RCAF Test (Diamond Mesh, Trapezoidal Cross Section)

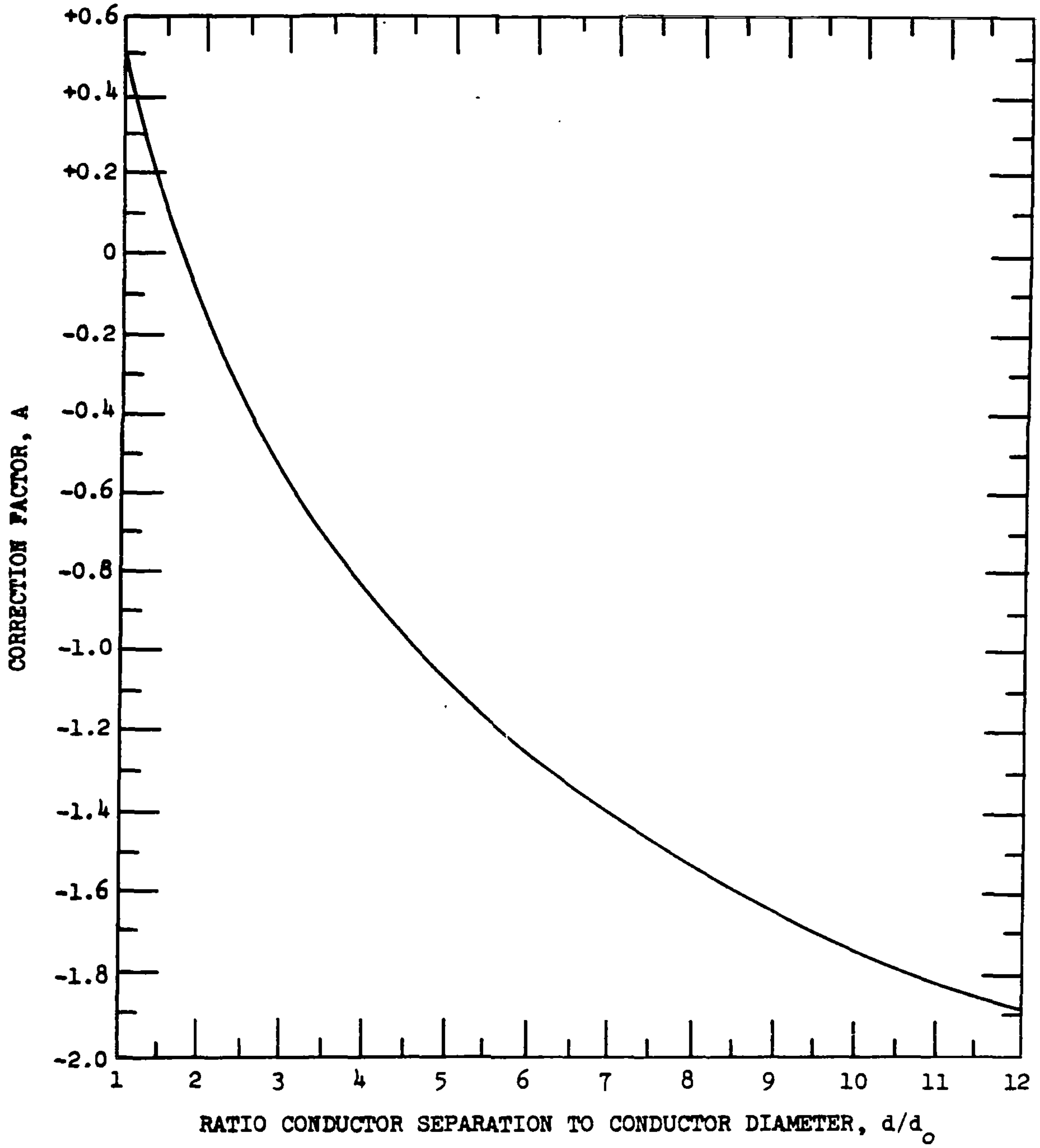

Figure 3. Empirical Constant A, a Correction Factor Used in Calculating the Inductance of a Solenoid

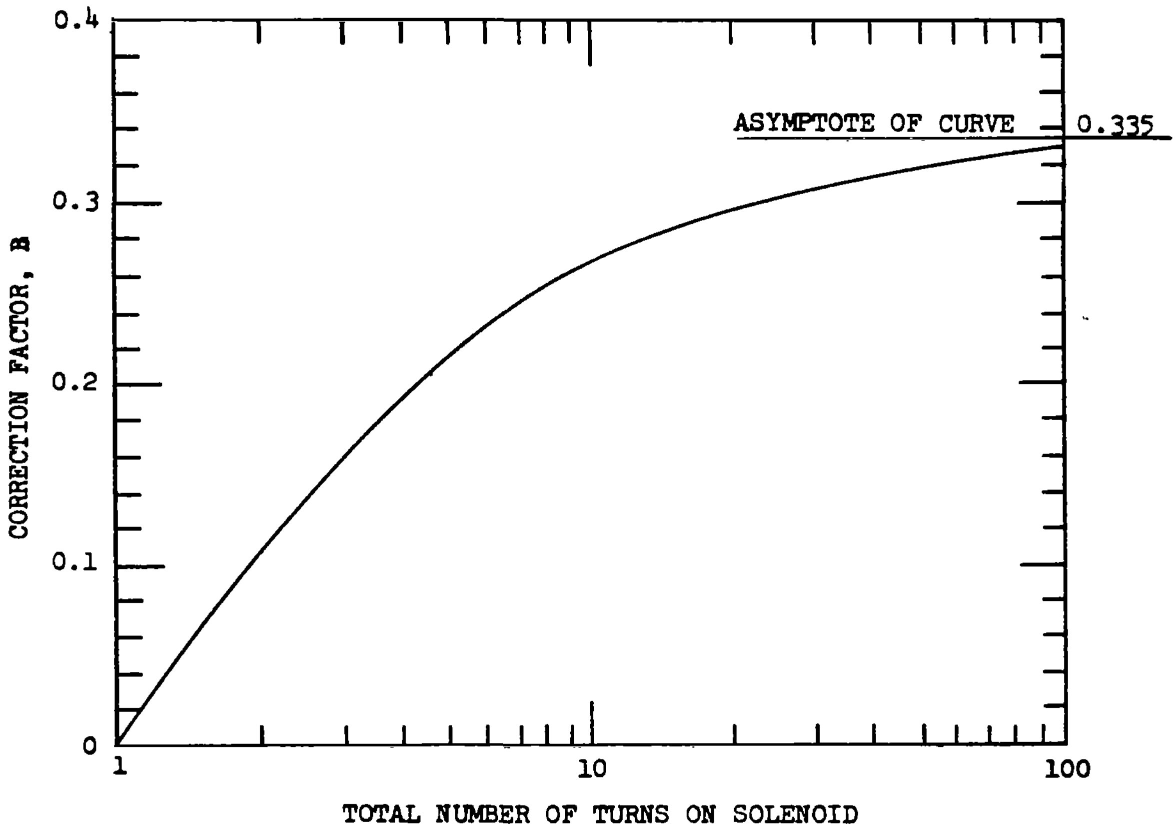

Figure 4. Empirical Constant B in Expression for the Inductance of a Solenoid

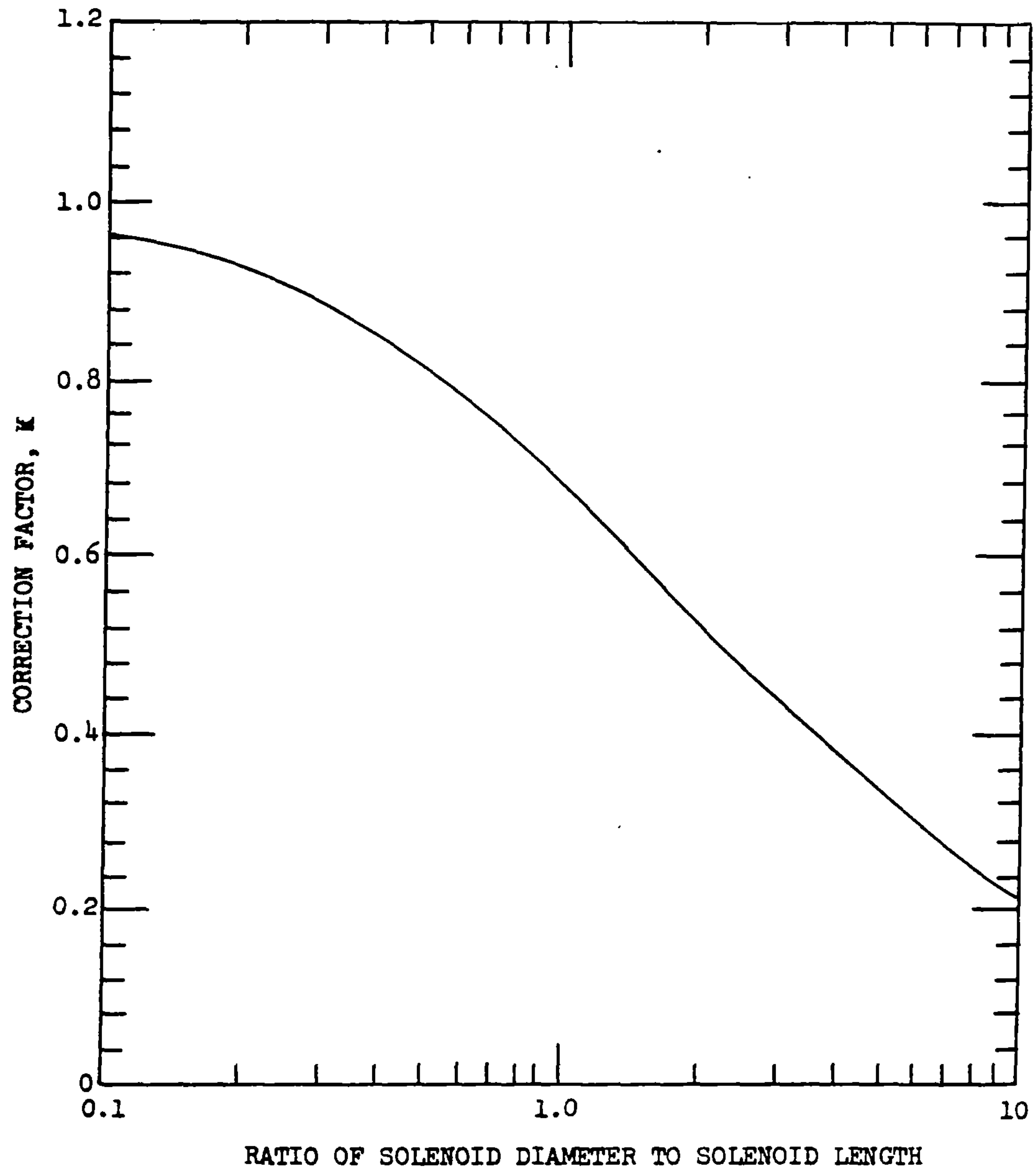

Figure 5. Factor K by Which Solenoid Inductance is Less Than That of a Solenoid of Infinite Length

The resistance per unit length of the mesh conductors is given by:

$$r_o = \frac{1}{\sigma} \frac{1}{\text{cross-sectional area}} = \frac{4}{\sigma \pi do^2}$$

The shielding factor η is divided into two parts, η_1 and η_2 where,

$$\eta_1 = \frac{-j Z_i}{\omega C} \quad \text{where} \quad C = \frac{K D \mu}{\pi d}$$

and $$\eta_2 = \frac{-2}{\pi} \frac{d}{D} (A+B)$$

Since η_1 is imaginary and η_2 is real;

$$\eta = [|\eta_1|^2 + |\eta_2|^2]^{1/2}$$

As an example problem, a calculation will be made for a copper mesh (σ = $5.6 \times 10^7 \Omega^{-1} m^{-1}$) with the mesh oriented vertically along the sides as in Figure 5(b) and a signal frequency of 10^4 cps. The following parameters are considered:

$D = 3.11$ meters

L = the length of the cage = 2.44 meters

$d = d_1 = 2.54 \times 10^{-2}$ meters

$\sigma = 5.6 \times 10^7 \Omega^{-1}$ meters^{-1}

$d_o = 6.32 \times 10^{-3}$ meters

The empirical constants are then determined from these parameters and Figures 3, 4 and 5.

$\frac{D}{L} = 1.274$, therefore $K = 0.63$ (Figure 5)

$\frac{d}{d_o} = 4.02$, therefore $A = -0.84$ (Figure 3)

$\frac{L}{d}$ = the number of turns = 96.1, therefore $B = 0.328$ (Figure 4)

The impedance condition $\frac{\gamma_o \ do}{4} \leq 1$ implies a condition on the

frequency : $f \leq 8.94 \times 10^2$, but as the problem is defined, $f > 8.94 \times 10^2$.

Therefore $Z_i = \frac{ro \quad \gamma o \quad do}{4}$

or $Z_i = \frac{4}{\sigma \pi do^2} \cdot \frac{\gamma o \quad do}{4} = 1.903 \times 10^{-3}\ \Omega/m$

$C = \mu \frac{KD}{\pi d} = 3.085 \times 10^{-5}$

Therefore $n_1 = -j \frac{Z_i}{2\pi f C} = -j\ 9.83 \times 10^{-4}$

and $n_2 = \frac{-2}{\pi} \frac{d}{D} (A + B) = 2.66 \times 10^{-3}$

so $|n| = [\ |n_1|^2 + |n_2|^2\ ]^{\frac{1}{2}} = 2.835 \times 10^{-3}$,

giving an attenuation of 51.0 db.

This theoretical development has shown a method to predict the shielding produced by a hollow metal mesh cube. The following section will relate the measurements that were performed to test this theory.

III. Shielding Measurements

The shielding measurements were performed in Ottawa, Canada by Air Force Weapons Laboratory personnel with the assistance of the Royal Canadian Air Force and Mr. I.G. Durand of Bell Telephone Laboratories.

A 10' x 10' x 16' square solenoid was wound on a wooden frame to supply the necessary test magnetic fields. CW fields at specific frequencies from 50 cps to 20 kc were generated in the solenoid. Field measurements were made with the solenoid empty; and with the 8' x 8' x 8' cages inside the solenoid.

The data obtained from the CW field tests were compared with theoretical calculations using formula developed by E. D. Sunde of Bell Telephone Laboratories in Section II.

Test Procedure

The test set up consisted of a 10' x 10' x 16' frame on which the field generating coils were wound. These coils formed an expanded 60 turn solenoid with a 3" spacing between turns (Figure 6). RG8 Cable, stripped of its outer shielding, was used in winding the solenoid.

The two 8' x 8' x 8' copper and aluminum test cubes were constructed by welding together 4' x 8' sheets of mesh with about a 4" overlap at the edges (Figure 7). The mesh construction was the same in both the copper and the aluminum cubes.

The CW fields were produced by energizing the field coils with a Hewlett-Packard signal generator. The generator fed the coils directly through a 1 ohm precision series resistor. By continuously monitoring the voltage across this resistor, the coil current was maintained at 0.01 amps for all test field frequencies. The fre-

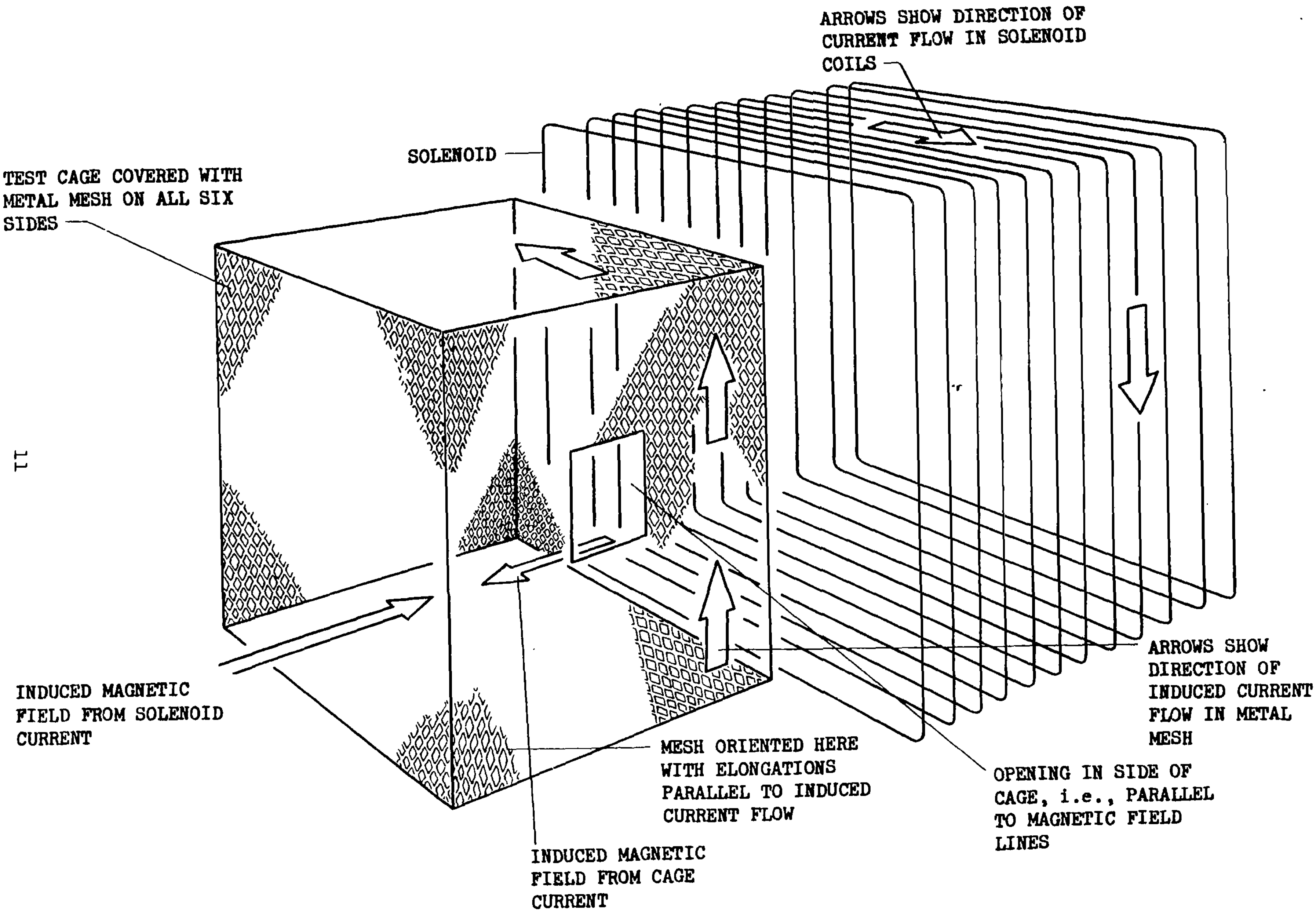

Figure 6. Aluminum Test Cage and Solenoid

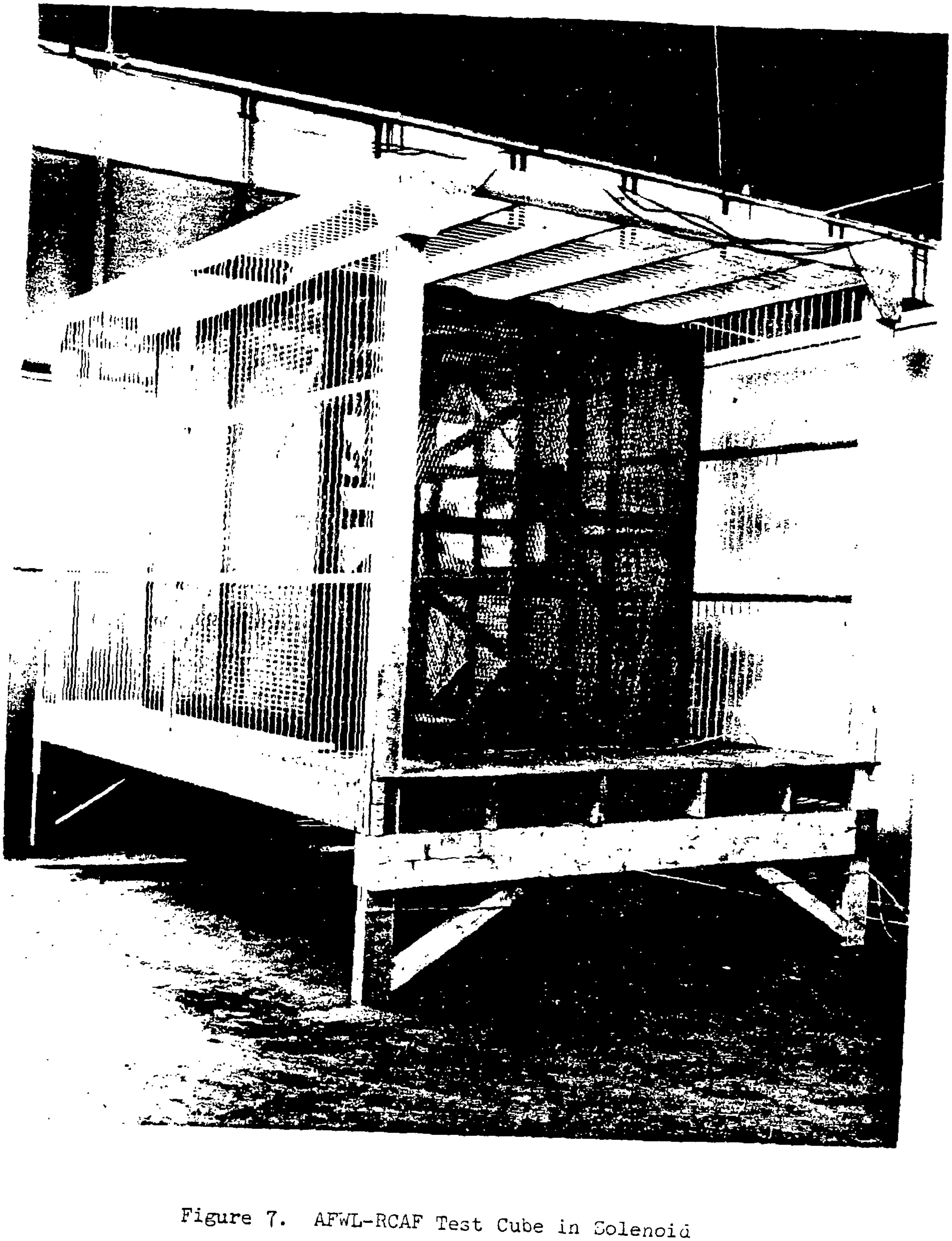

Figure 7. AFWL-RCAF Test Cube in Solenoid

quencies used were: 50, 100, 200, 400, 800, 1600, 3200, 6400, 12800, and 20000 cycles per second. The field measurements were performed using a Stoddart NM-40A Radio Field Intensity Meter and a General Radio Field Intensity Meter.

The magnetic field was mapped at various points throughout the solenoid for each test frequency. After mapping the unperturbed fields throughout the test enclosure, shielding tests were run on both metal cages (each placed exactly in the center of the test enclosure). Measurements were made in each case at a number of points within the cage, especially near areas where it was suspected large variations might occur.

The following list shows the tests conducted. It includes 7 separate CW tests on the aluminum cage and 4 separate CW tests on the copper cage.

Copper Mesh Tests

Test # 1 Copper

Copper test cube in field coil, mesh elongations parallel to current flow, with a 24" x 24" opening in front face (center of hole 4', 1.3', 5'; see Figure 8 for coordinate system used).

Test # 2 Copper

Copper test cube in field coil, mesh elongations parallel to current flow, with 24" x 24" hole closed with a square piece of copper mesh bolted over the hole in such a manner as to insure good electrical continuity with the remainder of the cage.

Test # 3 Copper

Copper test cube in field coil, mesh elongations parallel to current flow, with 24" x 24" galvanized steel duct 12' long entering test cube through an opening in front. (Center of opening 4', 1.3', 5'). The duct was insulated from the test cube (Figure 9).

The attenuation measurements were performed with the duct in three positions in the test cube.

Position #1 Duct all the way in (entering in front and going to the back wall of the test cube).

Position #2 Duct half way in the test cube.

Position #3 Duct 6" in the test cube.

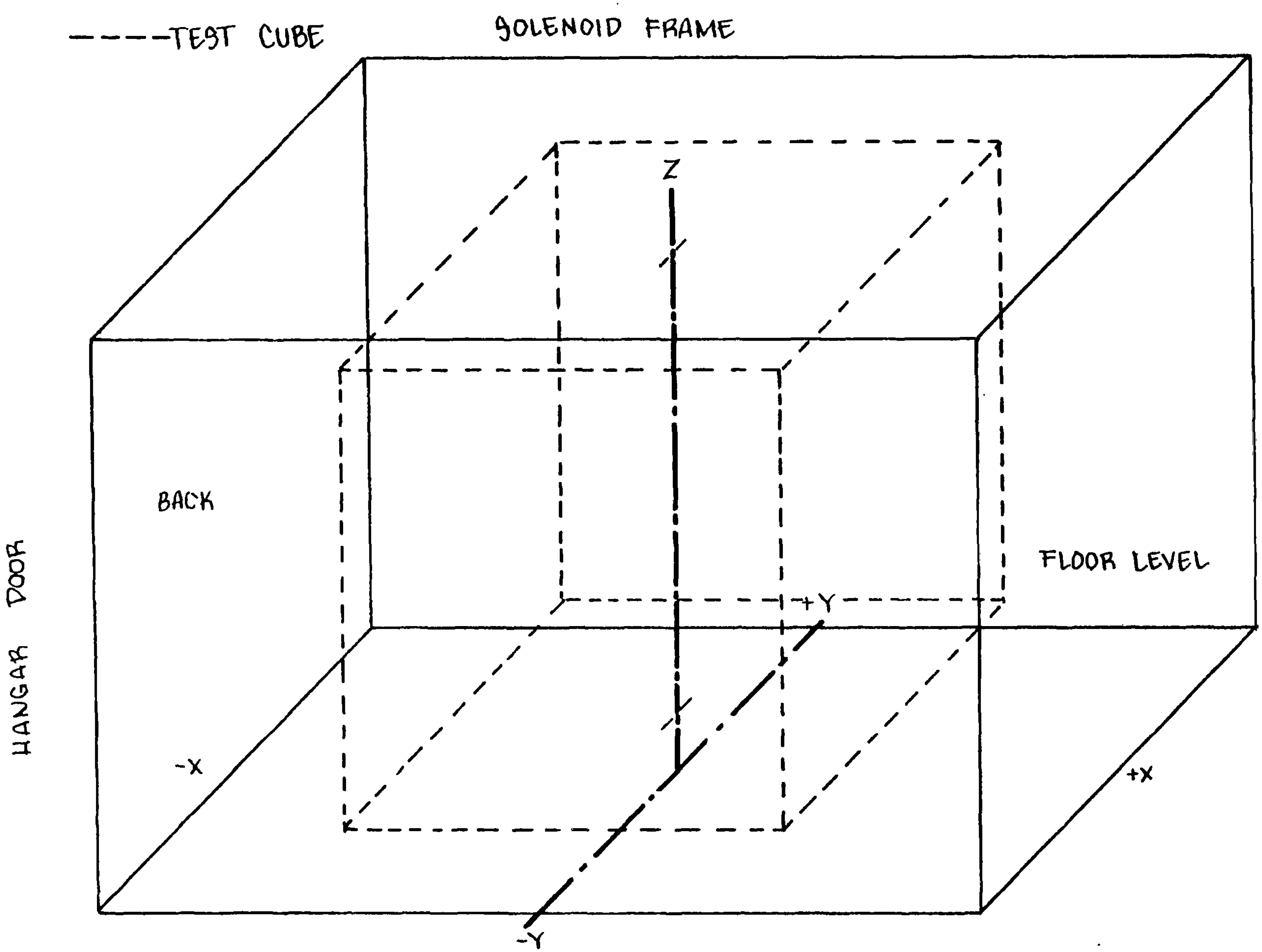

FIGURE 8 COORDINATES USED DURING TESTING

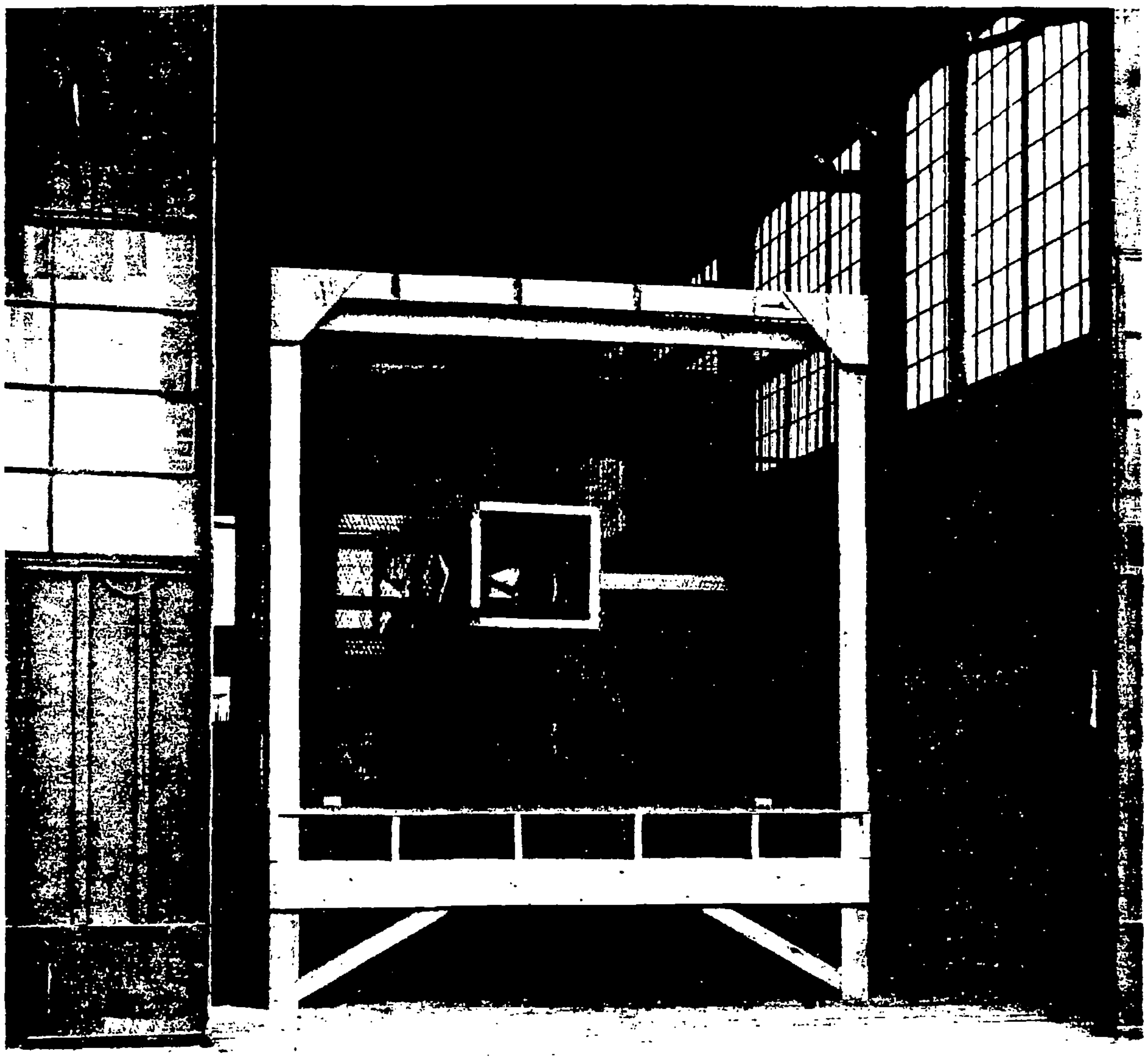

Figure 9. AFWL-RCAF Test Cube with Steel Duct in Opening

Test #4 Copper

Copper test cube in field coil, mesh elongations, parallel to current flow with a 24" x 24" galvanized steel duct half way in the test cube and welded to the test cube at entrance (Figure 9).

Aluminum Mesh Tests

Test #1 Aluminum

Aluminum test cube in field coil, mesh elongations parallel to current flow with 18" x 18" opening on the side (center of opening at 1', 4', 4').

Test #2 Aluminum

Aluminum test cube in field coil, mesh elongations perpendicular to current flow with 18" x 18" opening on the side (center of opening at -1', 4', 4').

Test #3 Aluminum

Aluminum test cube in field coil, mesh elongations parallel to current flow, with aluminum mesh welded over the opening on side of cube.

Test #4 Aluminum

Aluminum test cube in field coil, mesh elongations perpendicular to current flow, with aluminum mesh welded over the opening on side of cube.

Test # 5 Aluminum

Aluminum test cube in field coil, mesh elongations parallel to current flow with 18" x 18" opening on the side (center of opening 1', 4', 4'). A 10' x 10' field pick up loop was set up in the plane of the solenoid 7 feet forward of the center (center of pick up loop at 7', 0', 5'). Three tests were performed with this set up.

1. Measurements with the external field pick up coil entering through the opening going through the center of the test cube and connecting to the other side. The other end of the external field pick up coil left open.

2. Same as 1 except the other end of the external field pick up coil connected to the outside of the test cube at 4', 4', 5' (different connecting points on the outside of the test cube did not affect the readings).

3. Same as 2 except that the external field pick up coil was grounded at entrance to the test cube.

Test #6 Aluminum

Aluminum test cube (special side with 3/8" x 2 3/4" holes installed) in field coil, mesh elongations parallel to current flow.

Test #7 Aluminum

Aluminum test cube (special side 3/8" x 2 3/4" holes installed) in field coil, mesh elongations perpendicular to current flow.

These shielding measurements will now be compared with shielding calculations for the cubes from the theory of Section II, to determine if an adequate theory has been found to predict the shielding produced by cubical structures.

IV. Results

The mapping of the fields in the test enclosure in the absence of the test cages is given in Tables 1 & 2 for all test frequencies. Note that the fields at points within the volume of the test cages (marked by an asterisk) deviate only slightly from the fields measured at the geometric center of the enclosure 0', 0', 5'. Therefore, for comparison purposes to determine shielding data, for the different test configurations, the fields measured at the center will be considered uniform throughout volume to be occupied by the test cage, accurate to ± 1.5 db.

Similarly, whenever possible, the data to be considered for the measurement of general shielding given by a particular test configuration will be the data taken at the geometric center of the test cage (0', 0', 5'). In copper cage tests # 3 and #4, however, due to the presence of the metal duct the reading position within the cage will be considered which gives as a result the lowest shielding.

Figures 10 through 15 give the measured shielding results versus the theoretical curve, where applicable. Each of these graphs will now be analyzed to determine the effects introduced into the idealized shielding theory of Sunde by the various configurations.

Figure 10 for test #1, Copper Cage, shows that a 24" x 24" hole introduced in the side of the cage perpendicular to the magnetic field has little effect on the shielding effect of the cage, assuming of course that the wave length of the signal is much greater than the dimensions of the hole. This gives some indication that the main field attenuating currents are in the sides of the cage parallel to the field lines for a closed cage.

Comparison of this result with Figure 11 of Test #2, Copper Cage, did show that there was some loss of shielding due to the presence of the hole in Test #1. The closing up of the hole by bolting a piece of copper mesh to the edge over the hole increases the shielding from only slight at frequencies as low as 50 cps to only 3 db at high frequencies (10^4 cps or better). However, the effect of the hole is quite small compared to the 50 db total shielding given by the structure.

Figure 12 of Test #3, Copper Cage, shows the effect of placing a metal duct, insulated from the cage, at various positions through the above mentioned hole into the cage. The effect was nominal at best. The worst effect noted was with the duct in all the way entirely crossing the cage with the sensor at position 2', -2', 5'. The shielding drop at this position was from 2.5 - 4 db going from low to high frequency given by the structure. This result emphasizes the necessity of allowing about a 10 db safety factor when theoretically determining the necessary shielding for a given system which incorporates these wall penetrating devices.

Table 1 - Free Magnetic Field (db)

Stoddart Meter

Program: Field Mapping

Meter: Stoddart

	★											
Freq.	0,0,5	7,0,5	-7,0,5									
50	92	88	88									
100	98	94	93.5									
200	104	100.5	99.5									
400	110	106	105									
800	116	111.5	111									
1600	122.5	118.5	117.5									
3200	128.5	124	123.5									
6400	134	130	129.5									
12800	139	136	135									
20000												

★ Geometric center of test enclosure

Table 2 - Free Magnetic Field (db)

G/R Meter

Program: Field Mapping

Meter: G/R

	★						*	*	*			*
Freq.	0,0,5	7,0,5	7,0,1	7,4,1	7,4,5	7,4,5	4,4,5	4,0,5	4,0,1	5,4,1	5,4,5	4,4,1
50	78.5	81	81	79.5	81	89	78	79	78	78	78	77
100	68.5	72	71	70.5	71.5	79.5	68.5	69.5	68	68.5	69	68
200	68	71	71	69.5	71	79.5	67	69	67	68.5	67.5	67.5
400	58.5	62	61	60.5	61.5	69.5	57	58	59	58.5	58	57
800	54	57	56	55.5	56	64.5	53	54	54	54	53.5	52.5
1600	53	55	54.5	54	55	63	51.5	52.5	53	52.5	52.5	51.5
3200	44.5	48	47	46	47	55	43.5	44.5	45.5	45	44	43.5
6400	37	42	41	40	41	49	36	37	39.5	39	37	35.5
12800	33	36	35.5	35.5	36	44.5	32.5	32.5	35	34.5	33	32
20000	34	38	38	38	38	43	33.5	34	34.5	34.5	34.5	34

★ Geometric center of test enclosure

* These points are within volume occupied by test cage: fields deviate only slightly from the fields measured at the geometric center of the test enclosure.

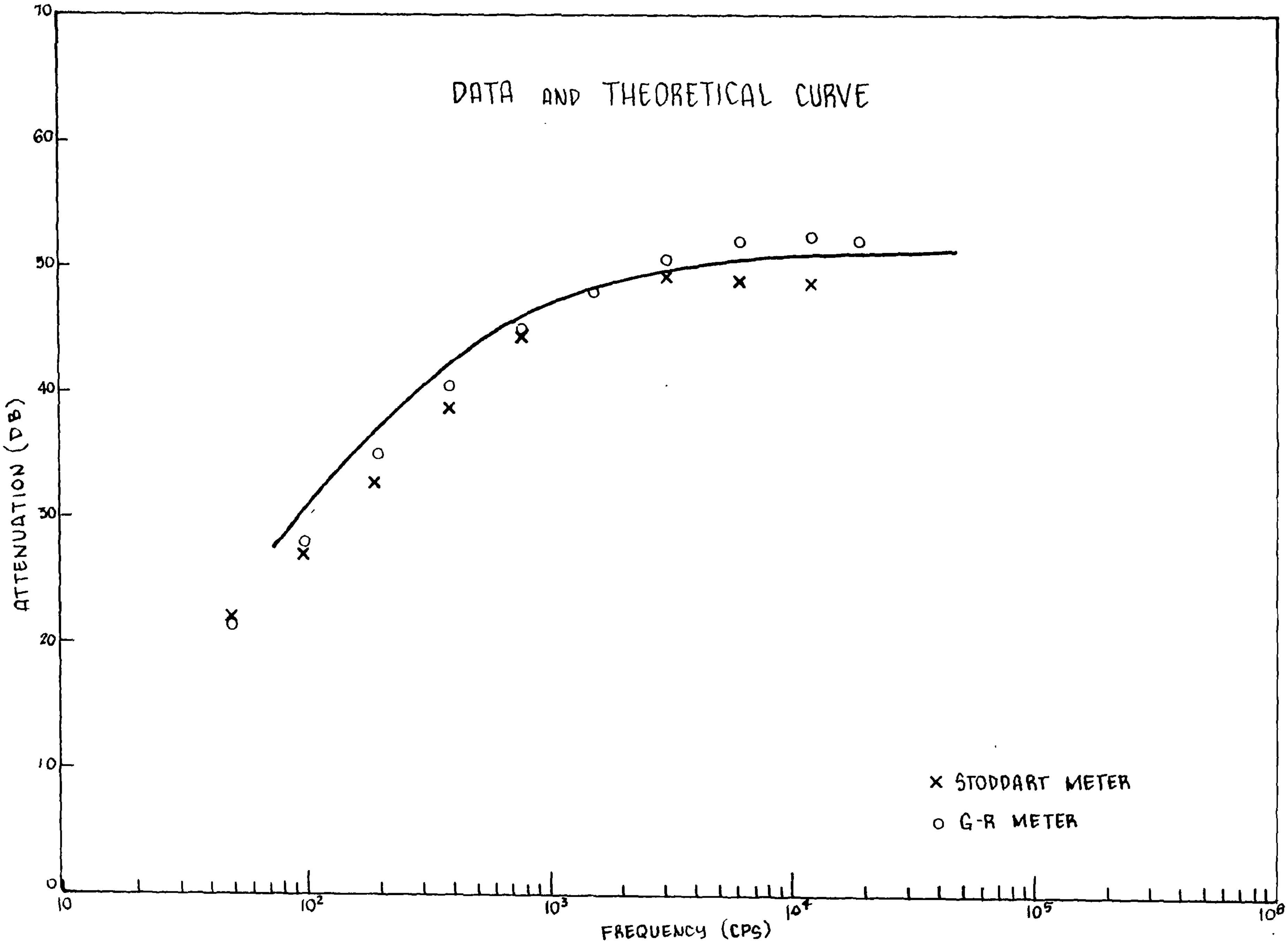

FIGURE 10 TEST 1 PER CUBE

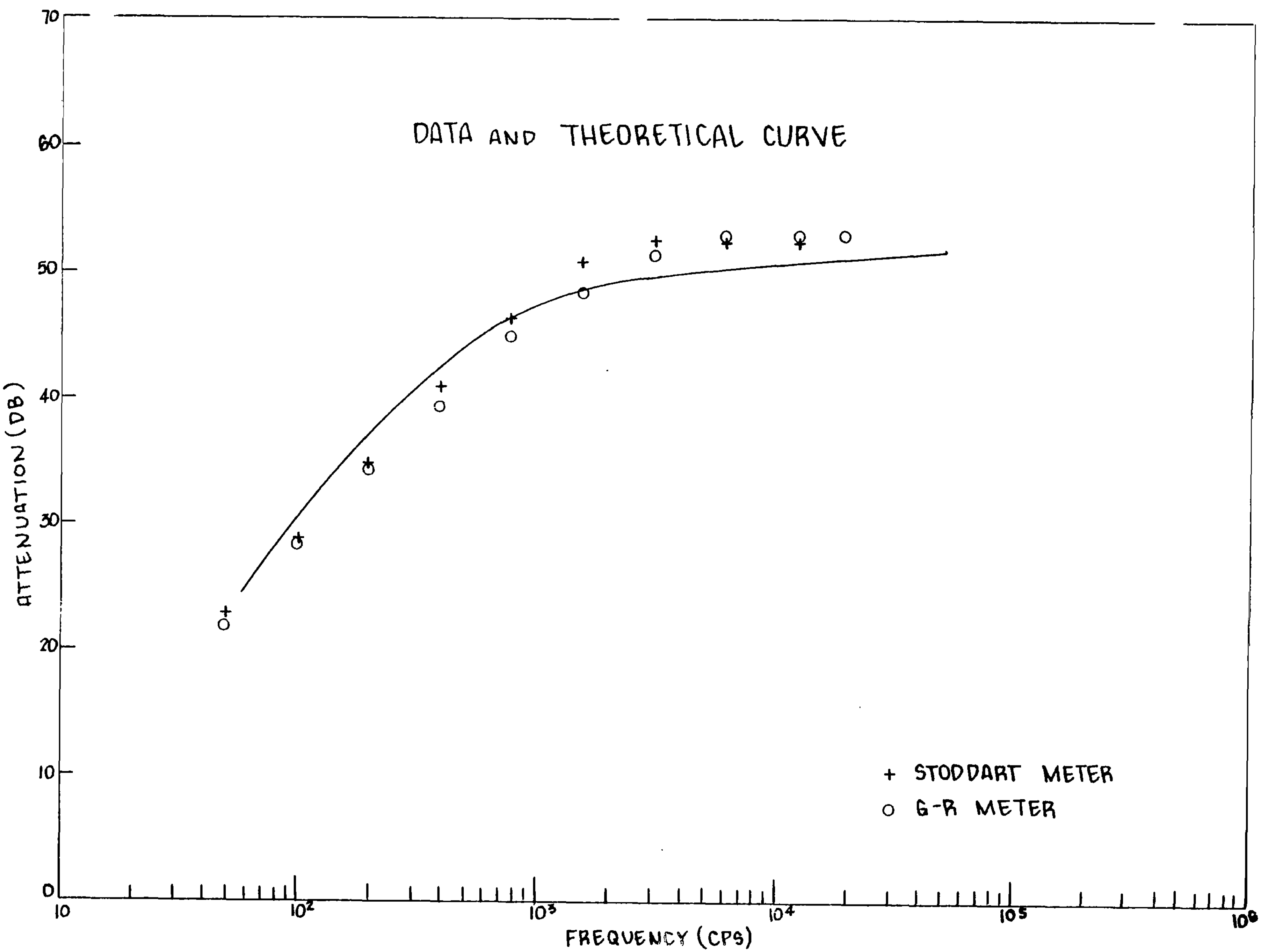

FIGURE 11 TEST # 2 COPPER CUBE

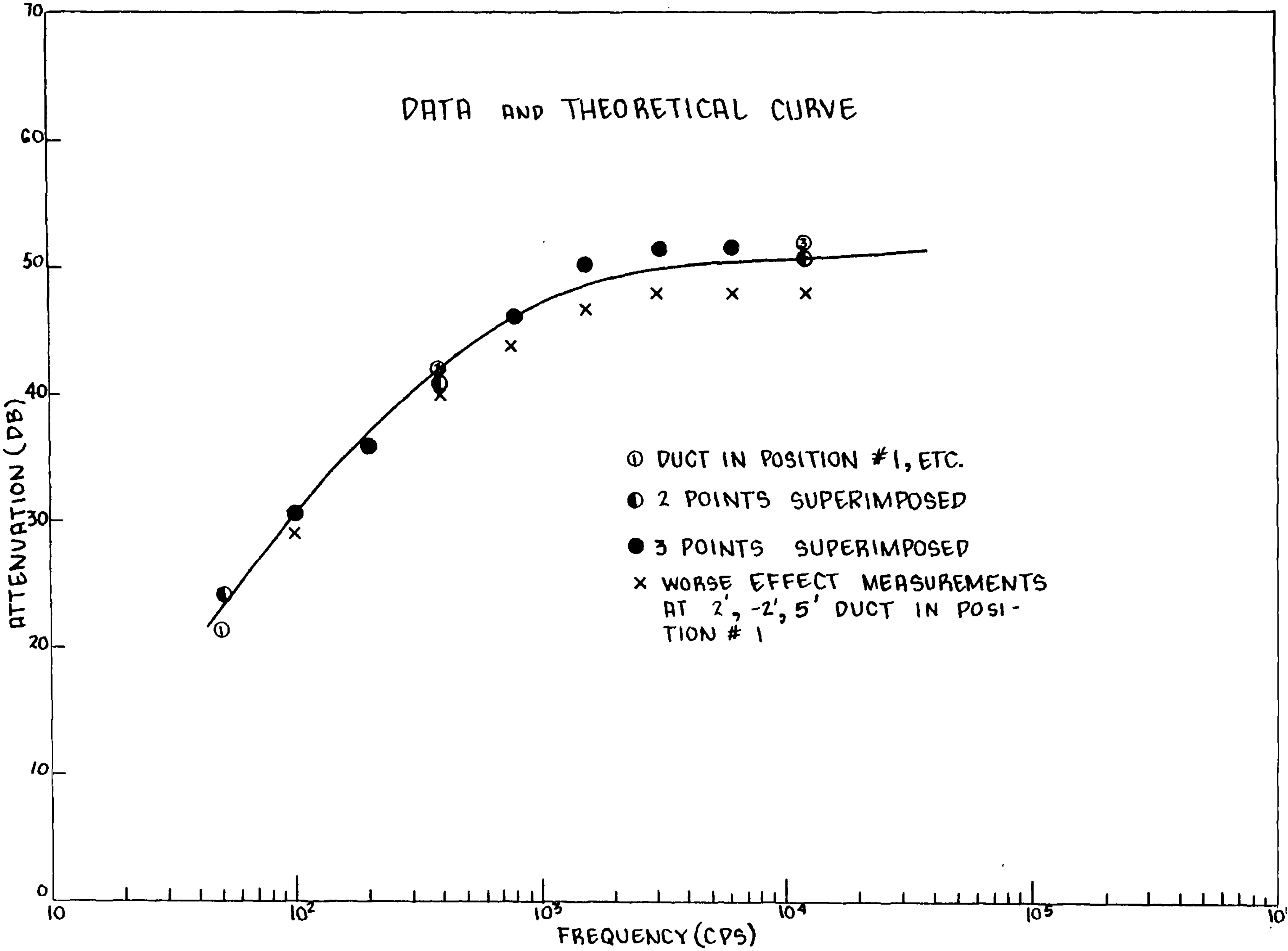

FIGURE 12 TEST #3 COPPER CUBE

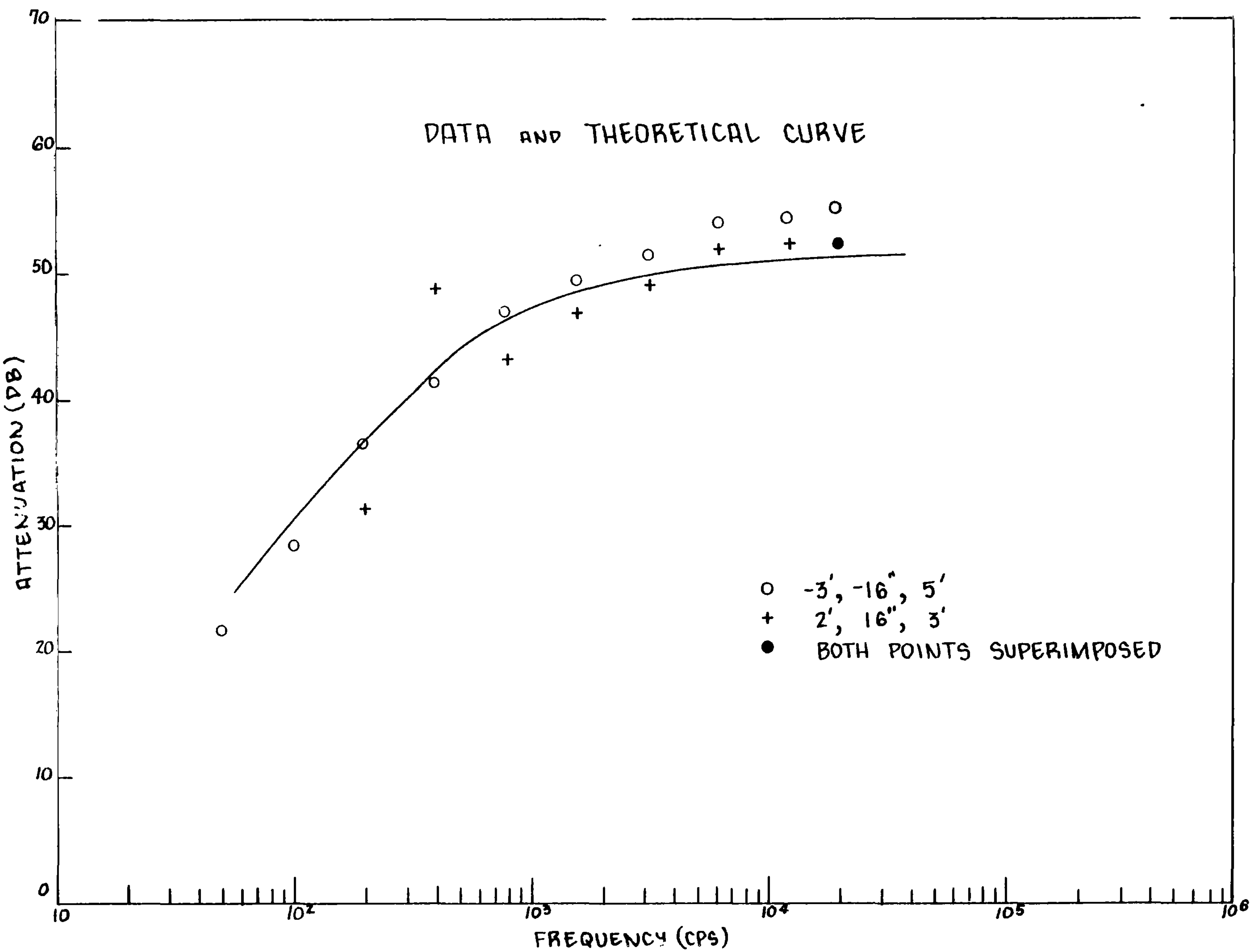

FIGURE 13 TEST # 4 COPPER CUBE

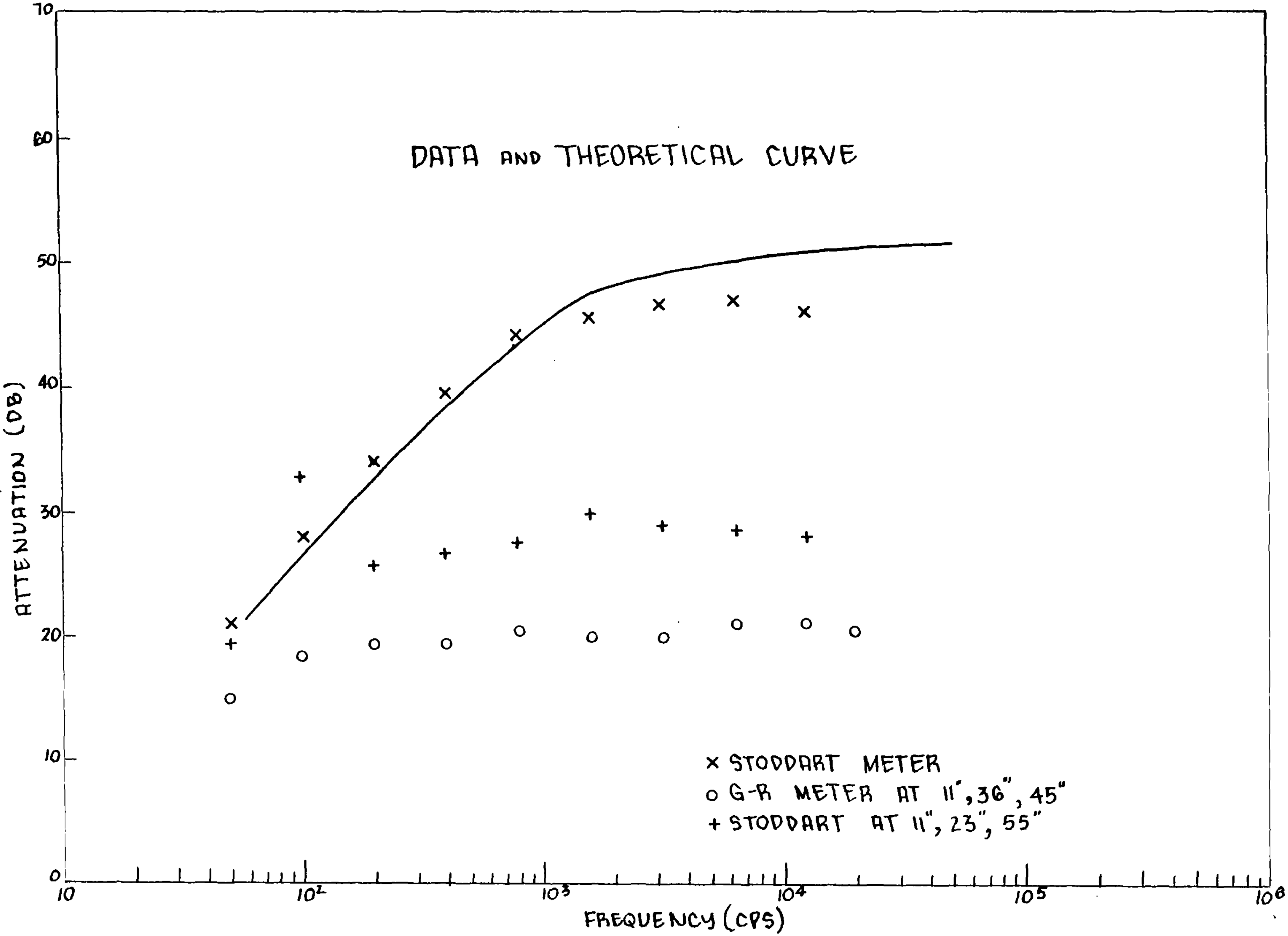

FIGURE 14 TEST #1 . CUBE

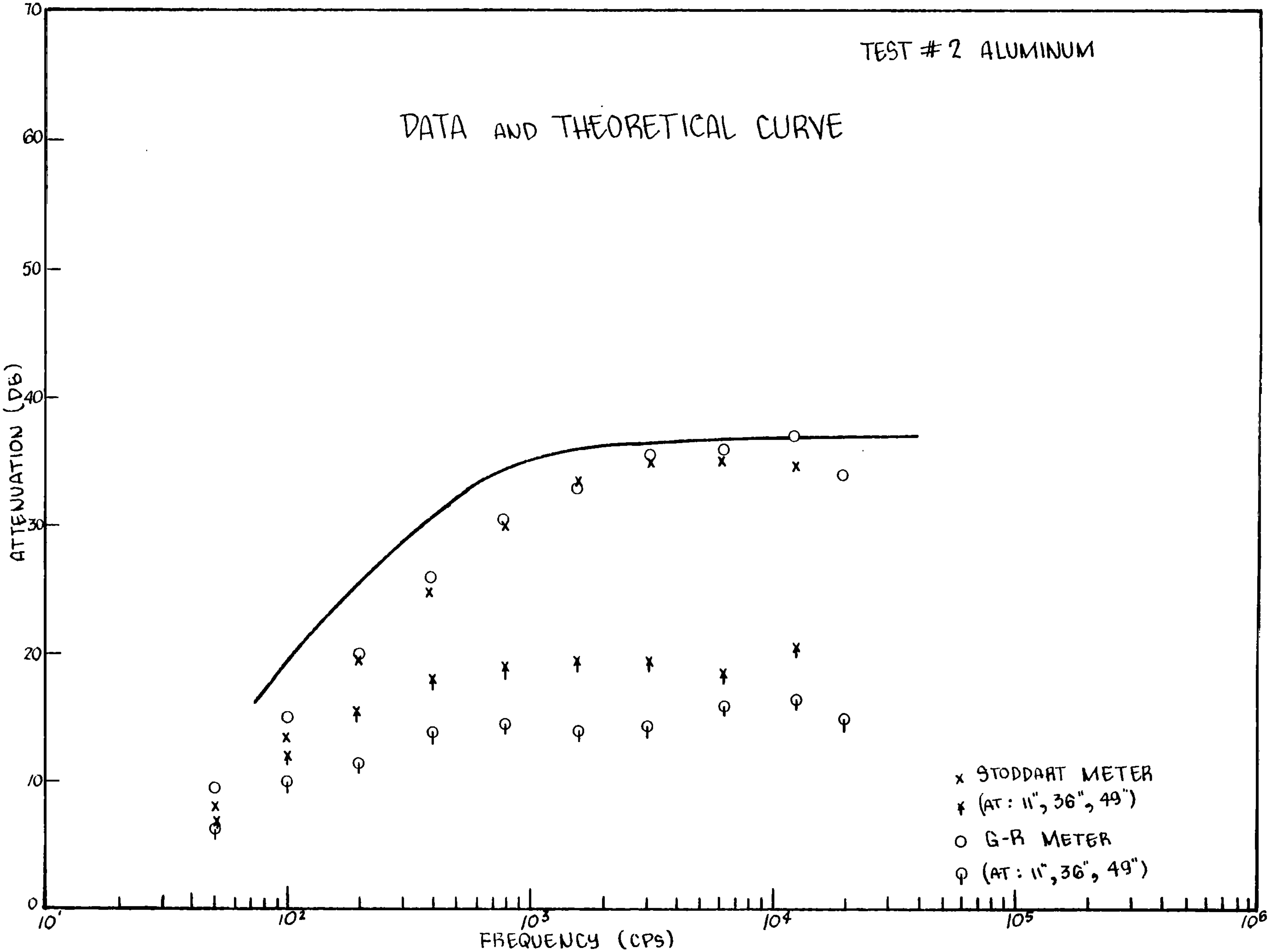

FIGURE 15 TEST # 2 AL CUBE

Figure 13 of Test #4, Copper Cage, shows the effect of welding the duct, placed in position #2, to the cage at the introductory hole. Except for a couple of questionable readings from the G-R meter, which can probably be attributed to operator error, the data shows little deviation from the theoretical calculation. In fact, the duct welded in this position shows roughly the same effect as Test #2, in which the hole was sealed. Although the effect is too small to make a quantitative evaluation, it may indicate the desirability of having sizeable conduit runs placed about any air vents entering the system, with the conduit welded to the wall shielding.

Figure 14 of Test #1, Aluminum Cage, shows the effect of having a sizeable hole in one of the sides of the cage parallel to the magnetic field lines. Note that the effect becomes noticeable only at higher frequencies. In particular, the hole affects the magnitude of the shielding level-off at higher frequencies. This result illustrates, at least at higher frequencies, that the higher percentage of attenuation current flows around the sides of the cage parallel to the field lines. The drop in this case is as much as 5 db. However, the total effect, as shown in Sunde's equations, will be dependent on the ratio of the size of the hole to the dimensions of the whole cage.

The measurements taken directly in front of the hole show a large drop in attenuation by as much as 30 db one foot inside the hole from that predicted by theory and down 25 db from the measurements taken at the center.

Data taken at -2', 2', 5' showed an increase in shielding even over the theoretical calculations by a few db. This may be due to current forced into this section of the cage by the presence of the hole in the adjoining section of the cage.

Figure 15 (Test #2, Aluminum Cage), shows the large change in shielding (around 13 db) that occurs when the conducting mesh has the long dimension of the holes placed perpendicular to the direction of current flow around the cage. That is, the long dimension is parallel to the magnetic field lines (See Figure 2). Sunde's theory accounts well for this change in shielding. Here too, however, the presence of the hole in the side, as in Test #1, produces results lower than the theoretical determination.

The measurements taken in front of the hole again show a large drop from the center measurements, as in Test #1. The drop is only 20 db below theory in this test, but this leaves only 15 db of attenuation left at this point.

Figure 16 (Test #3, Aluminum Cage), shows the change that occurs in the Test #1 data when a piece of aluminum mesh is welded over the opening in the side of the cage. The data here conforms nicely for all frequencies with the Sunde shielding theory.

Test #4, Aluminum Cage, (See Figure 17) is the counterpart of Test #2, with the hole welded as in Test #3. Here, as expected, the high frequency results conform nicely with the theory. However, the low frequency results are as much as 5 db below the theoretical estimate, although the falloff of the shielding with frequency is the same. This may be due to the theoretical approximation made of comparing the highly irregular shape of the mesh used with a simple square mesh.

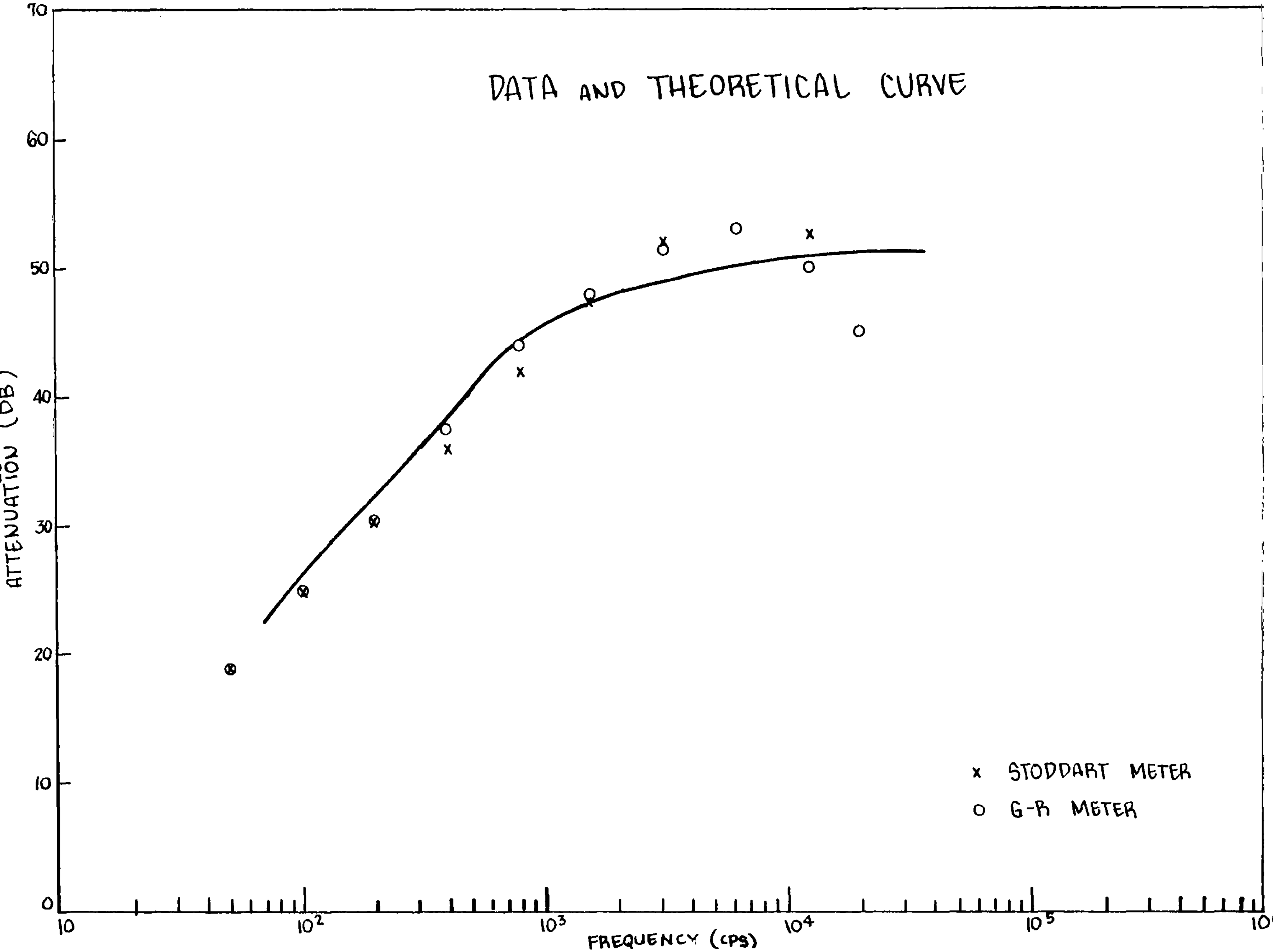

FIGURE 16 TEST 3 ALUMINUM CUBE

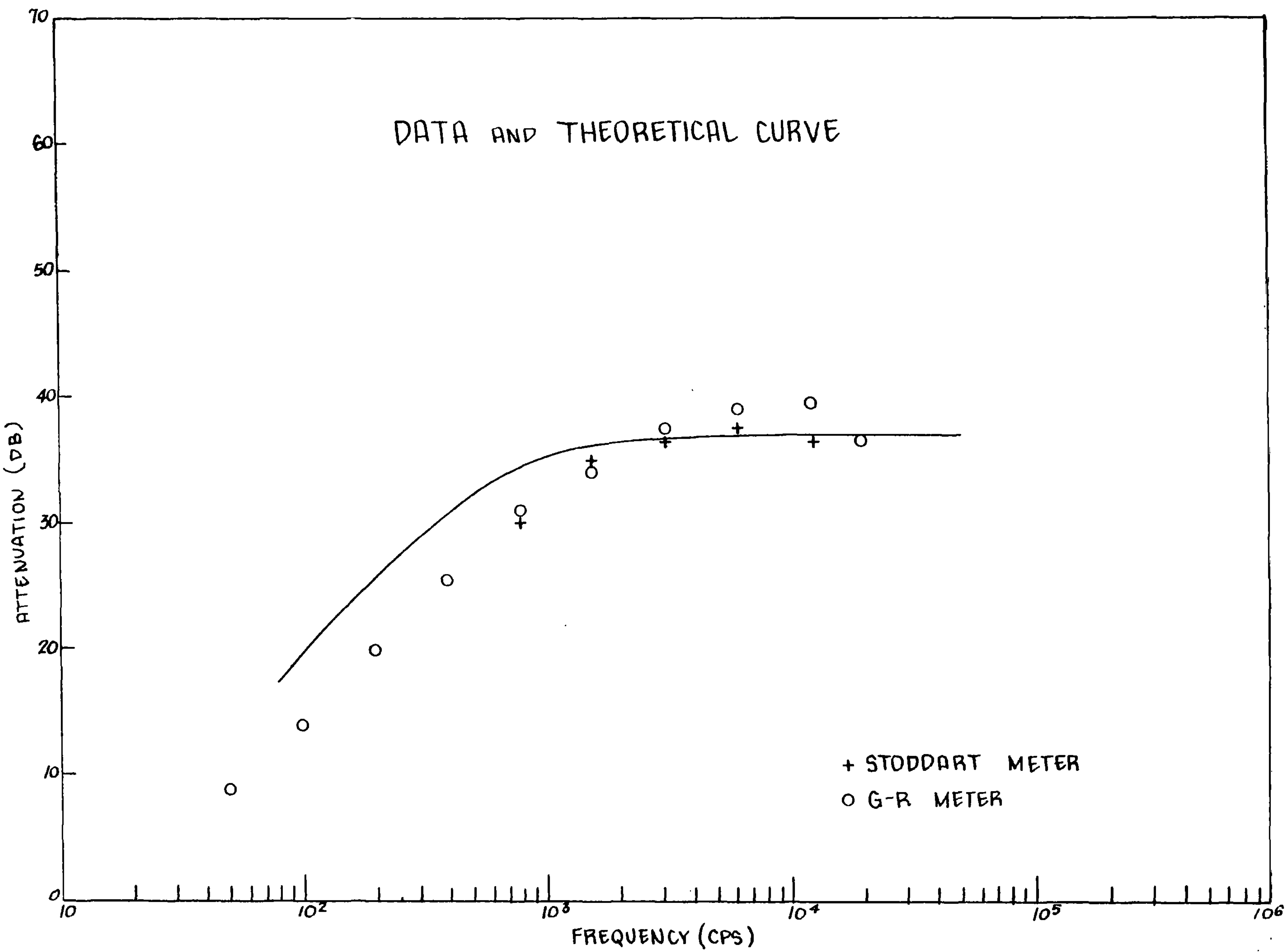

FIGURE 17 TEST #4 AL CUBE

With the mesh in the perpendicular orientation, this irregular path followed by the field-attenuating currents adds much to the impedance of the current path above that of the simple straight path of a square mesh.

Test #5, Aluminum Cage, (see Figure 18) illustrates the effect of a current carrying cable entering the cage. The current was produced by a pick up loop in the field outside the cage. Position #1, with no circuit established by the cable, gave the result with no current in the loop. As this test was accomplished with the hole of Tests #1 and #2 in the side of the cage, the result of Position #1 is comparable to that of Test #1. In Position #2, the cable circuit was completed, and the section of the cable running through the cage carried current. This current produced a field large enough to cut down the total effective shielding by 20 db at high frequencies, a sizeable loss. Position #3 shows the method of preventing shielding loss due to cables carrying high currents penetrating the shielding. By grounding out the cable at its point of entrance to the wall of the cage, the current was shorted through the cage and the shielding integrity of the cage was preserved. These results were not graphed. However, the results are within 1 db of the Position #1 results for all frequencies.

For Tests #6 and #7, Aluminum Cage, (Figures 19 and 20), one of the walls of the cage parallel to the field lines was replaced with a different aluminum mesh sheet. This mesh was a mesh with smaller area holes and thicker metal, which will produce a lower impedance path for the current. As the results for both tests show, this does improve the shielding by a few db. The improvement would be more noticeable if all the walls were replaced with the new mesh instead of just one wall. Test #7 has the long dimension of the mesh perpendicular to the current flow, as in Tests #2 and #4.

In all tests, several measurements were made at various corners and positions. The more interesting ones have been shown in each test. Except for tests where large holes were present in the cage, the measurements at the edges and in the corners of the cages showed little deviation from the measurements made at the center. At any rate, any deviation noted were not consistent from test to test, so little effective data can be obtained from these results. However, in no case were the measurements taken away from the center below those taken at the center (within the bounds of experimental error), except when the holes were present in the structure.

V. Summary

Sunde's shielding relation is determined mostly through the shielding of a finite length solenoid. That is, the walls of the cage perpendicular to the field lines are not considered in the shielding analysis. The effects produced by the holes in each of the cages show this. Only the aluminum cage, with its hole in a wall where the main current flow is occuring, has a noticeable deviation from the theory and from the results taken with the hole sealed shut with mesh. Therefore, Sunde's approach in his theory is justified in these tests.

By analyzing this theory, the shielding factor η , defined by Sunde, is seen to be proportional to the ratio of the conductor spacing to the conductor thickness. This was illustrated at least to a small degree in tests #6 and #7, Aluminum Cage, where a smaller spaced and larger conductor thickness type mesh was used on one wall of the cage.

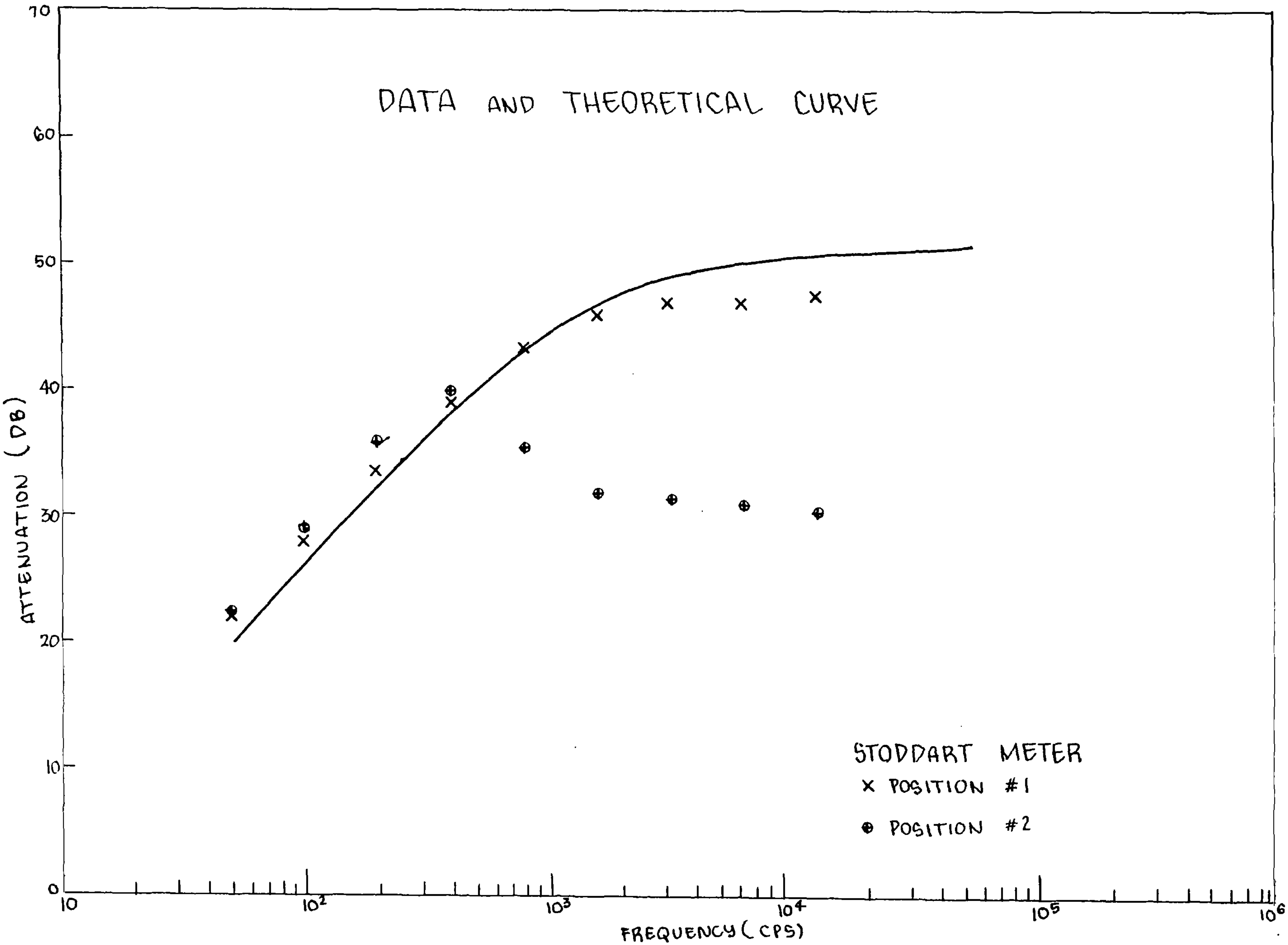

FIGURE 18 TEST 5 AL CUBE

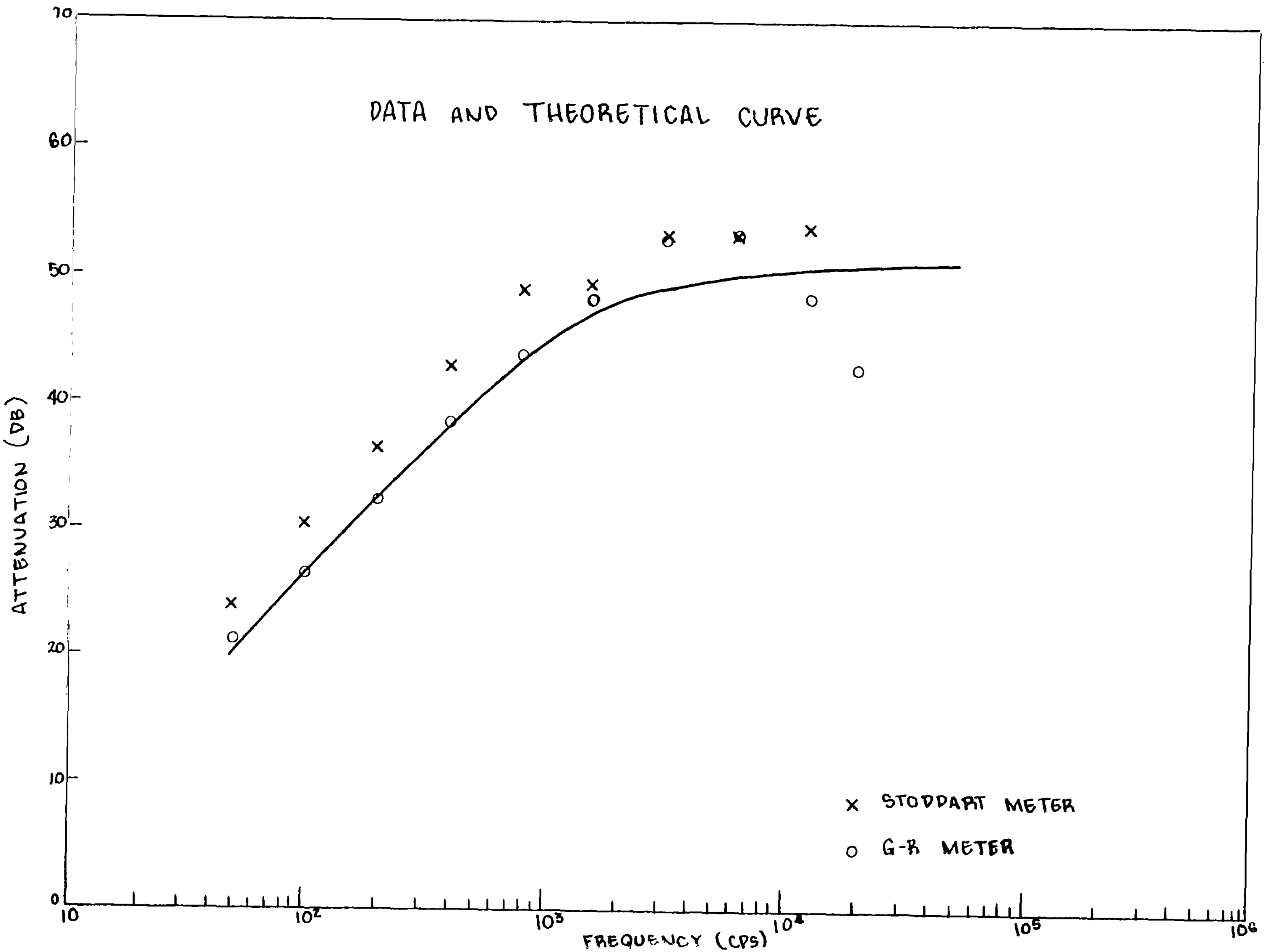

FIGURE 19 TEST 6 AL CUBE

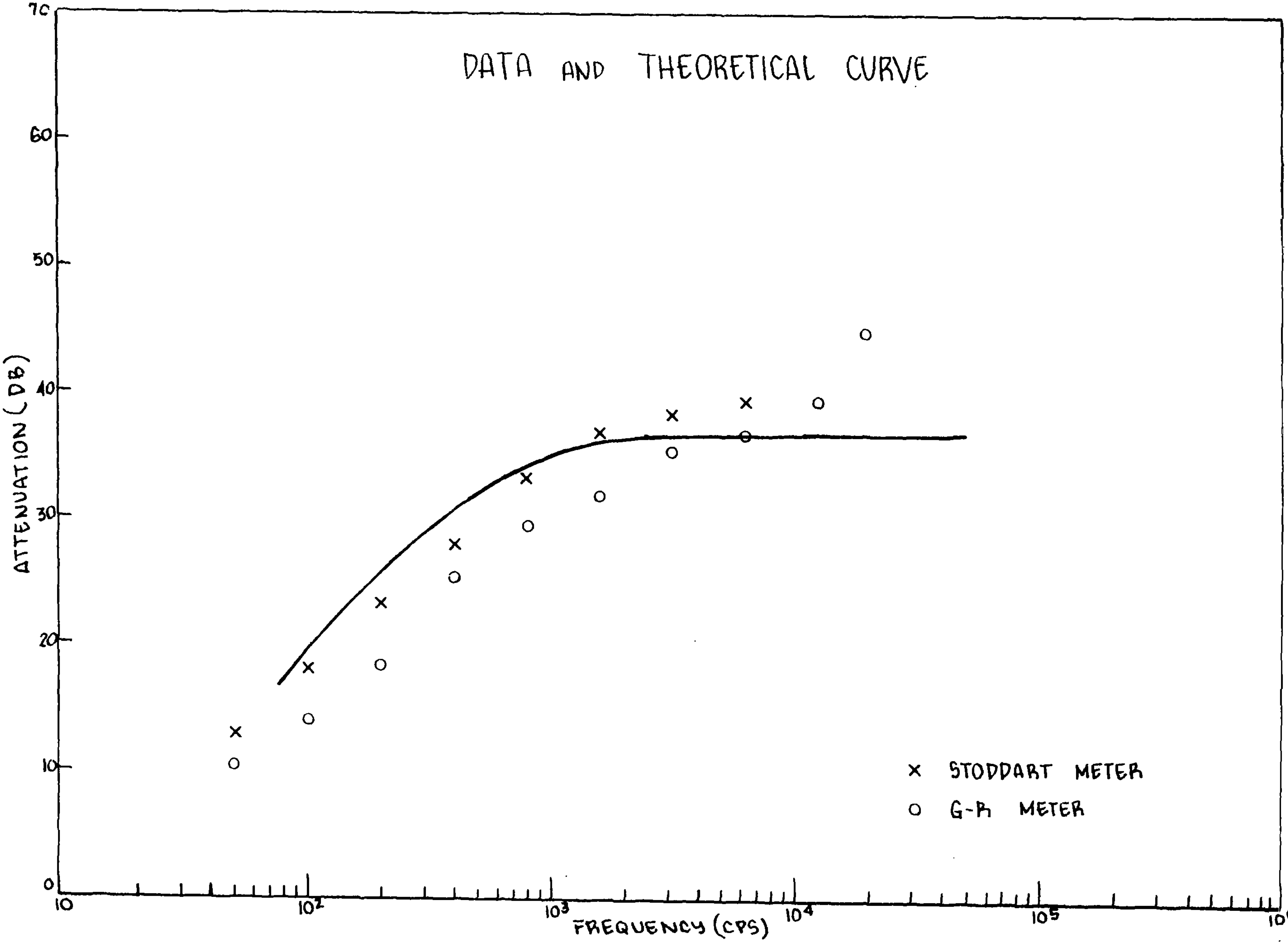

FIGURE 20 TEST # 7 AL CUBE

Test #5, Aluminum Cage, illustrated the necessity of grounding any incoming cables to the wall shielding to prevent the cable from circumventing the shielding.

Finally, Tests #2, #4, and #7, Aluminum Cage, showed that, for an irregular or oblong shaped mesh, the long dimension of the mesh must be placed parallel to the direction of the current flow about the shielded area. That is, the long dimension must be placed perpendicular to the direction of the expected magnetic field for best shielding results.